

Surface critical exponents at a uniaxial Lifshitz point

Michel Pleimling

Institut für Theoretische Physik I, Universität Erlangen-Nürnberg, Staudtstrasse 7B3, D – 91058 Erlangen, Germany

Using Monte Carlo techniques, the surface critical behaviour of three-dimensional semi-infinite ANNNI models with different surface orientations with respect to the axis of competing interactions is investigated. Special attention is thereby paid to the surface criticality at the bulk uniaxial Lifshitz point encountered in this model. The presented Monte Carlo results show that the mean-field description of semi-infinite ANNNI models is qualitatively correct. Lifshitz point surface critical exponents at the ordinary transition are found to depend on the surface orientation. At the special transition point, however, no clear dependency of the critical exponents on the surface orientation is revealed. The values of the surface critical exponents presented in this study are the first estimates available beyond mean-field theory.

I. INTRODUCTION

Critical phenomena at surfaces have been extensively studied theoretically during the last three decades.^{1–3} The surface phase diagram of the three-dimensional semi-infinite Ising model with only nearest neighbor couplings is well established. Introducing two different ferromagnetic interactions depending on whether the neighboring spins are both located at the surface, $J_s \geq 0$, or not, $J_b > 0$, two typical scenarios are encountered. If the ratio of the surface coupling J_s to the bulk coupling J_b , $r = J_s/J_b$, is smaller than a critical value, $r_{sp} \approx 1.50$ for the simple cubic lattice,^{4,5} the system undergoes at the bulk critical temperature T_c an ordinary transition, with the bulk and surface ordering occurring at the same temperature. Beyond this critical value one first observes the surface transition where the surface alone orders at a temperature $T_s > T_c$, followed by the extraordinary transition of the bulk at T_c . At the critical ratio r_{sp} , the special transition point is encountered, displaying critical properties distinct from those of the ordinary or the surface transition. The critical exponents of the different surface universality classes are known with rather high precision.⁶ However, far less is known on the surface critical behaviour of models with competing interactions which is the subject of the present paper.

The axial next-nearest-neighbor Ising (ANNNI) model^{7,8} is the best known of these models, its bulk properties being intensively investigated since many years. Here, competition between ferromagnetic nearest neighbor and antiferromagnetic next-nearest neighbor couplings takes place in one direction. The Hamiltonian of the three-dimensional version, defined on a cubic lattice, may then be written in the form

$$\mathcal{H} = -J_b \sum_{xyz} s_{xyz} (s_{(x+1)yz} + s_{x(y+1)z} + s_{xy(z+1)}) + \kappa_b J_b \sum_{xyz} s_{xyz} s_{xy(z+2)} \quad (1)$$

where $J_b > 0$ and $\kappa_b > 0$ are coupling constants. The

direction of competing interactions (here, the z -direction) is also called axial direction.

Spatially modulated phases due to competing interactions are observed, among others, in magnetic systems, alloys or ferroelectrics.^{8–12} Some compounds (as, for example, BCCD¹³ or NaV₂O₅¹⁴) display very rich phase diagrams with a multitude of commensurately or incommensurately modulated phases. A further remarkable feature of these systems is the possible existence of a special multicritical point called Lifshitz point.¹⁵ At a Lifshitz point, a disordered, a uniformly ordered and a periodically ordered phase become indistinguishable. Various systems have been shown to possess a Lifshitz point.^{16–19,14}

Recently, there has been renewed interest in the uniaxial Lifshitz point encountered in the phase diagram of the three-dimensional ANNNI model.^{20–27} This strongly anisotropic equilibrium critical point, located at $\kappa_b^L = 0.270 \pm 0.004$ and $k_B T_c^L / J_b = 3.7475 \pm 0.0005$,²⁷ is characterized by the anisotropy exponent $\theta = \nu_{\parallel}^L / \nu_{\perp}^L$ where ν_{\parallel}^L and ν_{\perp}^L are the exponents of the bulk correlation lengths parallel and perpendicular to the z -axis. The value $\theta \approx 0.49$ has been obtained in a second-order ϵ -expansion.^{22,24} Recent thorough determinations of Lifshitz point critical exponents using different techniques (field-theoretical calculations^{22,24} and Monte Carlo methods²⁷) have yielded excellent agreement. In addition, the scaling of the spin-spin correlator at the Lifshitz point was determined²⁷ and its form shown to agree with the prediction resulting from a generalization of conformal invariance to the strongly anisotropic scaling at the Lifshitz point.²⁸

Whereas the properties of the bulk ANNNI model are well established, far less is known about the behaviour of the ANNNI model in the presence of surfaces. Early Monte Carlo studies^{29,30} investigated ANNNI samples with free surfaces but did not pay special attention to surface properties as they were exclusively interested in bulk behaviour. Thin ANNNI films with free surfaces were studied recently and they were shown to present a dis-

tinct phase diagram for every film thickness.³¹ An early attempt to study surface critical behaviour near the Lifshitz point was undertaken by Gumbs³² in the framework of mean-field theory. A much more elaborated mean-field treatment of the semi-infinite ANNNI model was presented recently by Binder, Frisch, and Kimball.^{33,34} They considered two different surface orientations with respect to the axis of competing interactions: surfaces oriented perpendicular³³ or parallel³⁴ to this axis. For both cases the mean-field surface critical exponents at the Lifshitz points were determined and two different sets of critical exponents were obtained. This dependency of the critical behaviour on the surface orientation may be explained by the anisotropic scaling at the Lifshitz point. These authors also predicted the existence of a surface transition at the Lifshitz point where only the surface orders, in variance with Gumbs³² who claimed that at the Lifshitz point the surface could not order before the bulk. It is worth noting that no results beyond mean-field theory are available on the surface critical behaviour of the ANNNI model close to the Lifshitz point.

In this paper I present the first Monte Carlo study of the surface critical behaviour at the uniaxial Lifshitz point encountered in the ANNNI model. This study uses a cluster flip algorithm, especially designed for simulating models with competing interactions, which has been successfully employed in a recent investigation of the bulk ANNNI model.²⁷

The paper is organized in the following way. The next Section is devoted to the presentation of semi-infinite ANNNI models with two different surface orientations. Some details of the numerical method are also presented. Section III deals with surfaces perpendicular to the axis of competing interactions, paying special attention to the surface phase diagram and to the determination of surface critical exponents. Surfaces oriented parallel to this special direction are treated in Section IV. A short summary and outlook conclude the paper.

II. MODELS AND METHOD

Due to the anisotropy of the ANNNI model, surfaces with different orientations are not equivalent. The two surface orientations with respect to the axial direction considered in this paper are the followings (see Figure 1): surfaces perpendicular to the axis of competing interactions (case A) and surfaces parallel to this axis (case B). The same orientations were treated in recent mean-field studies.^{33,34}

For case A modified surface couplings with strength J_s connecting neighboring surface spins are introduced in addition to the usual ANNNI interactions, see Eq. (1) and Figure 1a. Three different scenarios have to be distinguished, depending on the value of the bulk competition parameter κ_b . When κ_b is smaller than the Lifshitz point value κ_b^L , the bulk undergoes a second order

phase transition between the disordered high temperature phase and the ordered, ferromagnetic, low temperature phase at the critical temperature $T_c(\kappa_b)$. This phase transition belongs to the universality class of the 3D Ising model. Consequently, the surface phase diagram will resemble that of the 3D semi-infinite Ising model, with a possible shift of the location of the special transition point, $r_{sp}(\kappa_b)$, as function of κ_b .³³ At the Lifshitz point, $\kappa_b = \kappa_b^L$, the recent mean-field treatment yields a surface phase diagram for the semi-infinite ANNNI model similar to the Ising model, but with critical exponents which differ from those of the Ising model. The conjectured existence³³ of a surface transition at the Lifshitz point, and therefore of a special transition point, is in agreement with the Monte Carlo results presented in the next Section. Finally, for strong axial next-nearest neighbor bulk couplings, $\kappa_b > \kappa_b^L$, the bulk phase transition belongs to the universality class of the 3D XY model. Therefore, for weak surface couplings, the ordinary transition critical behaviour should be identical to that of the three-dimensional semi-infinite XY model,³⁵ whereas for strong surface couplings the surface effectively decouples from the bulk and a two-dimensional bulk Ising critical behaviour is expected at the surface transition. These two critical lines meet at a multicritical point which should have interesting properties. However, I will in this study not consider the latter case as I am mainly interested in the surface critical behaviour at the Lifshitz point.

Case B with surfaces oriented parallel to the axial direction (see Figure 1b) is the most interesting but also the most demanding case. Introducing modified nearest neighbor, J_s , and axial next-nearest neighbor couplings, $\kappa_s \geq 0$, in the surface layer leads to intriguing and very complex situations. For example, a multicritical point shows up where an ordinary transition with a modulated bulk meets a surface transition to a floating incommensurate phase in the surface layer. In this study I will not discuss these peculiarities but concentrate exclusively on the case $\kappa_s \leq \kappa_b^L$. For these values of the surface competition parameter κ_s the corresponding two-dimensional ANNNI model presents a transition, belonging to the 2D Ising universality class, from the disordered phase to the low temperature ferromagnetic phase.³⁶

Surface quantities are determined by simulating ANNNI films consisting of $L_x \times L_y \times L_z$ spins, with free boundary conditions perpendicular to the surfaces and periodic boundary conditions otherwise. Hence, for case A the system consists of L_z layers with $L_x \times L_y$ spins per layer, whereas for case B the samples are formed by L_y layers containing $L_x \times L_z$ spins. The semi-infinite models are then obtained in the limit $L_x, L_y, L_z \rightarrow \infty$. Some care is needed when choosing the shape of the finite ANNNI films in the vicinity of the Lifshitz point. On the one hand, the special finite-size effects coming from the anisotropic scaling at this point³⁷ are best taken into account²⁷ by choosing anisotropic samples with an increased number of sites perpendicular to the axial direc-

tion. On the other hand, computation of surface quantities is usually done by simulating samples where the linear dimension of the surfaces exceeds the film thickness.³⁸ This does not pose any problem for case A, as here the axial direction coincides with the direction perpendicular to the surfaces. Therefore, for this case, systems of anisotropic shape with L_z layers and L_x^2 spins per layer are simulated, L_z ranging from 10 to 120 and L_x from 10 to 60. For case B, however, surfaces are parallel to the axial direction. In order to balance the competing finite-size effects, I have chosen to simulate cubes with L_x^3 spins, L_x ranging from 10 to 80. For comparison, a few simulations have also been done for samples with anisotropic shapes.

Critical phenomena are best studied numerically with non-local Monte Carlo methods. Recently, we proposed a cluster-flip algorithm, based on the one-cluster flip algorithm of Wolff,³⁹ especially designed for simulating spin systems with competing interactions.^{27,40} Below, this algorithm, which combines the cluster algorithm approaches for systems with long-range ferromagnetic couplings⁴¹ with that for systems with nearest neighbor random couplings,⁴² is reformulated in order to take modified surface couplings into account.

Let i be a lattice site characterized by the spin s_i and already belonging to the cluster we iteratively build up. A nearest neighbor site j with spin s_j is added to the cluster with probability

$$\frac{1}{2} (1 + \text{sign}(s_i s_j)) (1 - \exp[-2J_s/(k_B T)]) \quad (2)$$

if sites i and j are both located in the surface layer, and with probability

$$\frac{1}{2} (1 + \text{sign}(s_i s_j)) (1 - \exp[-2J_b/(k_B T)]) \quad (3)$$

otherwise. A lattice site k with spin s_k axial next-nearest neighbor to i is included with probability

$$\frac{1}{2} (1 - \text{sign}(s_i s_k)) (1 - \exp[-2J_s \kappa_s/(k_B T)]) \quad (4)$$

for case B if both spins are surface spins, and with probability

$$\frac{1}{2} (1 - \text{sign}(s_i s_k)) (1 - \exp[-2J_b \kappa_b/(k_B T)]) \quad (5)$$

otherwise. The final cluster, which is flipped as a whole, presents two peculiarities which are worth mentioning.⁴⁰ First, it contains spins of both signs, in variance with the Wolff cluster method, where all spins belonging to a cluster to be flipped have the same sign. Second, the cluster spins are not always connected by nearest neighbor bonds, which is again different from the traditional cluster flip method. This algorithm works well in the vicinity of the Lifshitz point, as demonstrated in the recent numerical study of the bulk Lifshitz point critical behaviour.²⁷

During the simulation, layer-dependent quantities are computed. I discuss these quantities here only for case A, the corresponding quantities for case B are obtained by replacing z by y and L_z by L_y . Of great interest when studying surface properties are the magnetization per layer

$$m(z) = \frac{1}{L_x L_y} \left\langle \left| \sum_{xy} s_{xyz} \right| \right\rangle \quad (6)$$

and the susceptibility per layer

$$\chi(z) = \frac{L_x L_y}{k_B T} \left[\left\langle \left(\frac{1}{L_x L_y} \sum_{xy} s_{xyz} \right)^2 \right\rangle - (m(z))^2 \right]. \quad (7)$$

The surface magnetization is then $m_1 = m(z=1) = m(z=L_z)$, whereas the response of the surface magnetization to a surface field is $\chi_{11} = \chi(z=1) = \chi(z=L_z)$. From the profiles $m(z)$ and $\chi(z)$ one also obtains the surface excess quantities

$$m_s = \sum_{z=1} (m_b - m(z)) \quad (8)$$

and

$$\chi_s = \sum_{z=1} (\chi_b - \chi(z)) \quad (9)$$

where m_b and χ_b are the bulk magnetization and the bulk susceptibility. The response of the surface to a bulk field, χ_1 , the energy, the specific heat, and the Binder cumulant have also been computed.

Thermal averages are extracted by generating, after equilibration, 5×10^5 clusters, and error bars are obtained by averaging over at least ten different realizations using different random numbers.

III. SURFACES PERPENDICULAR TO THE AXIAL DIRECTION

Semi-infinite ANNNI models with surfaces oriented perpendicular to the direction of competing interactions exhibit a crossover from Ising surface critical behaviour for $\kappa_b = 0$ to Lifshitz point surface criticality for $\kappa_b = \kappa_b^L$. For the purpose of studying this crossover, simulations were not only done for the value of κ_b at the Lifshitz point, $\kappa_b^L = 0.27$, but also at $\kappa_b = 0.15$ and $\kappa_b = 0.24$. The corresponding critical temperatures are listed in Table I. Note that the same values of κ_b have been used in a study of ANNNI bulk critical behaviour.⁴³

Various values of the surface coupling strength, J_s , have been considered, with J_s ranging from 0 to $3J_b$. The resulting surface phase diagrams are displayed in Figure 2, together with the corresponding phase diagram of the semi-infinite Ising model, $\kappa_b = 0$. The horizontal lines indicate the bulk critical temperatures which decrease with

increasing κ_b . One also observes a shift of the location of the special transition point to lower values of $r = J_s/J_b$ for larger values of the competition parameter κ_b , in accordance with the recent mean-field results.³³ This shift is mainly due to the decrease of the bulk critical temperature. The different surface transition lines in Figure 2 merge for $J_s \gg J_b$ and form one line independent of the value of κ_b . This follows from the fact that for very strong surface couplings the surface effectively decouples from the bulk. At the Lifshitz point value $\kappa_b = 0.27$, the phase diagram is also similar to the Ising case, with an ordinary transition, a surface transition, an extraordinary transition, and a special transition point. This is in agreement with the mean-field treatment of Ref.³³, but disagrees with the results obtained in Ref.³². Based on our data, the special transition point of the semi-infinite ANNNI model at the Lifshitz point is located at $r_{sp}^L = 1.15 \pm 0.05$.

Crossover phenomena showing up in the surface magnetization may be analysed by plotting the effective exponent

$$\beta_{1,eff} = d \ln m_1 / d \ln t \quad (10)$$

where $t = (T_c - T)/T_c$ is the reduced temperature. On approaching T_c , $t \rightarrow 0$, $\beta_{1,eff}$ becomes the critical exponent β_1 of the surface magnetization. In the following, data unaffected by finite-size effects are usually displayed, finite-size dependences being circumvented by adjusting the size of the sample.³⁸

Effective surface magnetization exponents obtained for $\kappa_b = 0, 0.15$, and 0.24 , with $J_s = J_b$ are shown in Figure 3. Clearly, for a fixed value of t , $\beta_{1,eff}$ decreases with increasing κ_b . In the limit $t \rightarrow 0$, however, the effective exponents all tend asymptotically to the critical surface magnetization exponent $\beta_1 \approx 0.80$ of the semi-infinite Ising model at the ordinary transition,³⁸ in accordance with the Ising character of the ANNNI bulk transition for $\kappa_b < \kappa_b^L$.⁴³ The observed increase of the corrections to scaling with κ_b reflects not only the closer proximity of the bulk Lifshitz point but also the reduced distance of $r = J_s/J_b = 1$ to the special transition point $r_{sp}(\kappa_b)$. This is illustrated in Figure 3 by the data obtained for $\kappa_b = 0.24$ with $J_s = 0.5J_b$ where corrections to scaling are greatly reduced compared to the case $J_s = J_b$.

Some of the results obtained for $\kappa_b = \kappa_b^L$, with $r < r_{sp}^L$, are displayed in Figures 4 and 5. For this choice of the interactions, the surface undergoes an ordinary transition at the Lifshitz point critical temperature T_c^L . Both the magnetization per layer, shown in Figure 4, and the susceptibility per layer (not shown) vary non-monotonously close to T_c^L . Whereas a non-monotonic behaviour of the layer susceptibility is also observed close to the ordinary transition in thick Ising films, the layer magnetization increases monotonically in Ising films from its surface value to the bulk value.³⁸ The non-monotonic behaviour of the layer magnetization close to the Lifshitz point ordinary transition may be explained in the following way. Inside the bulk the value of the magnetization mainly results

from the balancing of competing influences in axial direction. Close to the surface, however, some negative contributions are missing, which then yields a tendency to stronger local ordering, resulting in a maximum of the layer magnetization near the surface. Similar non-monotonic profiles also show up in the semi-infinite critical Ising model in the presence of a weak surface field.⁴⁴ It should be noted that in our case the appearance of non-monotonic profiles depends strongly on the value of the competition parameter κ_b . This behaviour is not observed for the studied values of κ_b smaller than κ_b^L . For $\kappa_b = \kappa_b^L$ the maximum in the magnetization profile shows up for all values of the surface coupling J_s leading to the ordinary transition. When the temperature is increased, the maxima both of the layer magnetization and of the layer susceptibility are shifted towards the center of the system.

The surface magnetizations and the corresponding effective exponents obtained for two different values of the coupling ratio J_s/J_b are compared in Figure 5. As expected, the amplitudes (see Figure 5a) and the corrections to scaling (see Figure 5b) differ. It is only close to T_c , for $t \leq 0.07$, that the effective exponents (and therefore the corrections to scaling) become identical. Furthermore, the effective exponents then vary almost linearly with temperature. A linear extrapolation yields the value $\beta_1^L = 0.618 \pm 0.005$ for the surface magnetization critical exponent at the Lifshitz point ordinary transition. This value is clearly smaller than the value $\beta_1 = 0.80 \pm 0.01$ obtained at the ordinary transition of the semi-infinite Ising model.³⁸ It is worth noting that mean-field approximation yields the common value $\beta_1^{MF} = 1$ for both cases.

Estimates of Lifshitz point surface critical exponents at the ordinary transition are gathered in Table II. Hereby, the critical exponent $\gamma_1^L = 0.84 \pm 0.05$ of the susceptibility χ_1 , i.e. of the response of the surface to a bulk field, can be obtained by analysing the corresponding effective exponent in the same manner as discussed previously. The response of the surface to a surface field, χ_{11} , however, is finite at T_c^L , with a cusp-like singularity when approaching the critical point from high temperatures. Instead of trying to extract the corresponding critical exponent γ_{11}^L directly from χ_{11} , it is easier to study the derivative $\chi'_{11} = d\chi_{11}/dT$ which in our case diverges on approach to the critical point with the power law $\chi'_{11} \sim (-t)^{-\gamma_{11}^L-1}$. This then yields the value -0.06 ± 0.02 for γ_{11}^L .

Further Lifshitz point surface critical exponents are obtained by analysing the power law behaviour of the excess quantities m_s and χ_s , see Eq. (8) and (9), close to the critical point: $m_s \sim t^{\beta_s^L}$ and $\chi_s \sim t^{-\gamma_s^L}$. Based on our data, the excess quantities critical exponents are estimated in the present case to be $\beta_s^L = -0.14 \pm 0.04$ and $\gamma_s^L = 1.69 \pm 0.07$.

A closer inspection of Table II reveals that various scaling relations are fulfilled, thus demonstrating the reliability of our estimates. Indeed, inserting the Lifshitz point bulk critical exponents $\gamma_b^L = 1.36 \pm 0.03$ and

$\beta_b^L = 0.238 \pm 0.005^{27}$ as well as $\nu_{\parallel}^L = 0.348$,²⁴ the following scaling relations are readily verified:

$$\beta_s^L = \beta_b^L - \nu_{\parallel}^L \quad (11)$$

$$\gamma_s^L = \gamma_b^L + \nu_{\parallel}^L \quad (12)$$

$$2\gamma_1^L - \gamma_{11}^L = \gamma_s^L \quad (13)$$

Lifshitz point surface quantities have also been studied near the special transition point with $J_s = 1.15J_b$, see above. At temperatures below T_c^L magnetization profiles are extremely flat: only very close to the surface does one observe a slow increase of the layer magnetization which reaches a maximum in the layer immediately below the surface layer. The surface magnetization itself is slightly smaller than the bulk magnetization. Estimated values of Lifshitz point surface critical exponents at the special transition point are listed in Table II. As both the bulk and the surface become critical at the special transition point, the responses of the surface to a bulk field as well as to a surface field diverge. The corresponding critical exponents are estimated to be $\gamma_{1,sp}^L = 1.28 \pm 0.08$ and $\gamma_{11,sp}^L = 0.76 \pm 0.05$ where effective exponents have again been analysed. For the surface magnetization critical exponent the value $\beta_{1,sp} = 0.22 \pm 0.02$ is obtained. Error bars given for the special transition point critical exponents include the uncertainty in the localisation of this multicritical point.

It is worth noting that the Lifshitz point surface critical exponent at the special transition point given in Table II agree within the error bars with the estimates^{45,6} of the corresponding exponents for the semi-infinite Ising model. The change from Ising to Lifshitz point bulk critical behaviour when $\kappa_b \rightarrow \kappa_b^L$ seems to have only a minor impact on the computed surface critical behaviour at the special transition point. However, this may not hold for the crossover exponent, which describes the merging of the surface transition line with this point,¹ as different values are obtained in mean-field approximation for the Ising and for the Lifshitz point case.³³ In the present work, no attempt was made to determine the crossover exponent.

IV. SURFACES PARALLEL TO THE AXIAL DIRECTION

Two different approaches have been chosen for studying the critical behaviour of surfaces oriented parallel to the axial direction. In the first approach the value of the surface competition parameter κ_s is set to zero so that only the strength of the surface nearest neighbor coupling J_s is varied. In the second approach the bulk and surface competition parameters have the same value, $\kappa_s = \kappa_b$, with J_s ranging from 0 to $6J_b$. Simulations done for the

latter case may be viewed as a preparatory work for the study of the more complex multicritical points mentioned in Section II. In this work I mainly discuss Lifshitz point surface criticality, i.e. $\kappa_b = \kappa_b^L$, at the ordinary transition and at the special transition point.

First one has to note that the critical value of the coupling ratio $r_{sp} = J_s/J_b$, needed for the surface to get critical by itself, now depends both on the bulk and on the surface competition parameters. For example, at the bulk Lifshitz point $r_{sp}^L = 1.75 \pm 0.05$ for $\kappa_s = 0$, whereas for $\kappa_s = \kappa_b^L$ the special transition point is tentatively located at $r_{sp}^L \approx 4.3$. This remarkable shift of the critical coupling ratio to larger values in the latter case may be explained by a stronger weakening of the effective surface couplings, due to the competing surface interactions, than of the effective bulk couplings.

At the bulk Lifshitz point, the magnetization per layer increases monotonically from its surface value to its bulk value, as shown in Figure 6. This is in marked contrast to the behaviour encountered when the surface is perpendicular to the axial direction, as discussed in the previous Section, see Figure 4. For the surface orientation considered here, the layers are parallel to the direction of competing interactions, so that no axial contributions are missing close to the surface and no tendency to stronger local ordering is expected.

Lifshitz point surface critical exponents at the ordinary transition, which have been computed in a similar way as for case A, are gathered in Table III. These values should be compared with the corresponding values of case A surfaces listed in Table II. Figure 7 shows effective exponents derived from the surface magnetizations obtained by simulating samples with different surface orientations. Clearly, both types of surfaces yield different asymptotic values β_1^L for the effective exponent, thus demonstrating that the values of surface critical exponents depend on the surface orientation. Different values are also obtained for the critical exponents γ_{11}^L , β_s^L , and γ_s^L . For γ_1^L the situation is not so clear as rather similar values follow from the analysis of effective exponents. One may note that mean-field theory yields for γ_1^L the same value for both surface orientations.^{33,34}

Whereas the scaling relation (13) is fulfilled independently of the orientation of the surface, the scaling relations (11) and (12) have to be modified for surfaces parallel to the axial direction. Indeed, the behaviour of excess quantities is governed close to a bulk critical point by the bulk correlation length along the direction perpendicular to the surface. The Lifshitz point being an anisotropic critical point characterized by two correlation lengths diverging with different critical exponents, ν_{\perp}^L respectively ν_{\parallel}^L has to be used for case B respectively A surfaces. This then yields for surfaces parallel to the axial direction the scaling relations

$$\beta_s^L = \beta_b^L - \nu_{\perp}^L \quad (14)$$

and

$$\gamma_s^L = \gamma_b^L + \nu_\perp^L. \quad (15)$$

Using $\nu_\perp^L = 0.709$,²⁴ a nice agreement with the numerical estimates for β_s^L and γ_s^L is observed.

I also studied the Lifshitz point surface critical behaviour of surfaces oriented parallel to the axial direction close to the special transition point, choosing $\kappa_s = 0$ and $J_s = 1.75J_b$, with $\kappa_b = \kappa_b^L$. The estimates for the critical exponents $\beta_{1,sp}^L$, $\gamma_{1,sp}^L$, and $\gamma_{11,sp}^L$ have been included in Table III. Again, the quoted error bars take into account the sample averaging as well as the uncertainty in the location of the special transition point. Interestingly, the values of the critical exponents are very similar to the values obtained for the other type of surfaces considered in Section III and quoted in Table II. This is a strong indication that at the bulk Lifshitz point the surface critical behaviour at the special transition point may not depend on the surface orientation.

V. CONCLUSION AND OUTLOOK

Whereas surface criticality of models with only ferromagnetic couplings has been the subject of numerous investigations, studies of surface critical behaviour in systems with competing interactions are very scarce. The aim of the present work is to fill some gaps by presenting the first Monte Carlo study of surface critical behaviour in semi-infinite three-dimensional ANNNI models, paying special attention to the ordinary transition as well as to the special transition point, both at the bulk Lifshitz point. Prior works^{32–34} exclusively focused on the mean-field treatment of this problem.

Overall, the numerical results, which have been obtained by studying different surface orientations with respect to the axis of competing interactions, are in qualitative agreement with results obtained in the recent mean-field treatments.^{33,34} The location of the special transition point is a function of the bulk competition parameter as well as of the surface competition parameter, when present. At the bulk Lifshitz point, the surface diagram is similar to that of the semi-infinite 3D Ising model, with a surface transition line ending in a special transition point. This is in accordance with recent mean-field results,^{33,34} but disagrees with the early treatment of Gumbs.³² Finally, at the bulk Lifshitz point, surface critical exponents at the ordinary transition depend on the orientation of the surface, as predicted by mean-field theory.

The main results of our study are the Monte Carlo estimates of surface critical exponents at the bulk Lifshitz point gathered in Tables II and III. This is the first time that values for these exponents have been determined numerically. Whereas at the ordinary transition surface critical exponents depend on the surface orientation, the computed values at the special transition point do not show a clear dependency on the orientation of the surface with respect to the axial direction. Furthermore,

these values agree rather well with the values obtained in the Ising model at the special transition point. In order to clarify the situation at this multicritical point renormalization group calculations are desirable. However, with regard to the immense technical difficulties already encountered in the field-theoretical computation of bulk critical exponents at the Lifshitz point,^{22–26} this seems to be a formidable task not easily achievable in the near future.

A host of open and interesting problems remains for future work. In the present study, surface criticality has only been investigated for values of the bulk competition parameter $\kappa_b \leq \kappa_b^L$, thus neglecting the interesting case when the bulk undergoes a phase transition to a modulated structure. Similarly, for surfaces parallel to the axial direction, the surface competition parameter κ_s has been chosen in such a way that at the surface transition a uniformly ordered phase appears in the surface layer. However, for large values of κ_s one will observe a surface transition to a floating incommensurate phase in the surface layer. Various interesting scenarios follow, one of the most interesting being a multicritical point where a surface transition line with a floating phase in the surface layer meets an ordinary transition line with a modulated bulk.

A further interesting question concerns the scaling form at the Lifshitz point of spin-spin correlation functions along and perpendicular to the surface. A recent generalization of conformal invariance to the strong anisotropic scaling at the Lifshitz point²⁸ has yielded predictions for the scaling form of bulk two-point correlators which were found to agree perfectly with Monte Carlo results.²⁷ Similarly, predictions for two-point correlation functions in semi-infinite systems at the Lifshitz point can be obtained in the framework of this theory and may then be compared to numerical data. Work along the sketched lines is planned for the future.

ACKNOWLEDGMENTS

I thank Malte Henkel for useful discussions, and him and Alfred Hüller for a critical reading of the manuscript.

¹ K. Binder, in *Phase Transitions and Critical Phenomena*, Volume 8 (C. Domb and J.L. Lebowitz, eds.), Academic Press, London, and New York (1983).

² H.W. Diehl, in *Phase Transitions and Critical Phenomena*, Volume 10 (C. Domb and J.L. Lebowitz, eds.), Academic Press, London, and New York (1986).

³ H.W. Diehl, *Int. J. Mod. Phys. B* **11**, 3503 (1997).

⁴ K. Binder and D.P. Landau, *Phys. Rev. Lett.* **52**, 318 (1984).

⁵ C. Ruge, S. Dunkelmann, F. Wagner, and J. Wulf, *J. Stat. Phys.* **73**, 293 (1993).

⁶ H.W. Diehl and M. Shpot, Nucl. Phys. B **528**, 595 (1998), and references therein.

⁷ R.J. Elliott, Phys. Rev. **124**, 346 (1961).

⁸ W. Selke, Phys. Rep. **170**, 213 (1988).

⁹ J.M. Yeomans, Solid State Physics **41**, 151 (1988).

¹⁰ H.Z. Cummins, Phys. Rep. **195**, 211 (1980).

¹¹ W. Selke, in *Phase Transitions and Critical Phenomena*, Vol.15, edited by C. Domb and J.L. Lebowitz (Academic Press, New York, 1992).

¹² B. Neubert, M. Pleimling, and R. Siems, Ferroelectrics **208-209**, 141 (1998).

¹³ G. Schaack and M. Le Maire, Ferroelectrics **208-209**, 1 (1998).

¹⁴ K. Ohwada et al., Phys. Rev. Lett. **87**, 086402 (2001).

¹⁵ R.M. Hornreich, M. Luban, and S. Shtrikman, Phys. Rev. Lett. **35**, 1678 (1975).

¹⁶ Y. Shapira, C.C. Becerra, N.F. Oliveira, and T.S. Chang, Phys. Rev. **B24**, 2780 (1981).

¹⁷ M. Škarabot, R. Blinc, I. Muševič, A. Rastegar, and Th. Rasing, Phys. Rev. **E61**, 3961 (2000).

¹⁸ Y.M. Vysochanskii and V.U. Slivka, Usp. Fiz. Nauk **162**, 139 (1992) [Sov. Phys. Usp. **35**, 123 (1992)].

¹⁹ A. Schröder, G. Aeppli, E. Bucher, R. Ramazashvili, and P. Coleman, Phys. Rev. Lett. **80**, 5623 (1998).

²⁰ C.C. Becerra, V. Bindilatti, and N.F. Oliveira, Jr., Phys. Rev. **B62**, 8965 (2000).

²¹ M.M. Leite, Phys. Rev. **B61**, 14691 (2000).

²² H.W. Diehl and M. Shpot, Phys. Rev. **B62**, 12338 (2000).

²³ L.C. de Albuquerque and M.M. Leite, J. Phys. A **34**, L327 (2001).

²⁴ M. Shpot and H.W. Diehl, Nucl. Phys. **B612**, 340 (2001).

²⁵ H.W. Diehl and M. Shpot, J. Phys. A **34**, 9101 (2001).

²⁶ M.M. Leite, hep-th/0109037.

²⁷ M. Pleimling and M. Henkel, Phys. Rev. Lett. **87**, 125702 (2001).

²⁸ M. Henkel, Phys. Rev. Lett. **78**, 1940 (1997).

²⁹ W. Selke and M.E. Fisher, Phys. Rev. **B20**, 257 (1979).

³⁰ E.B. Rasmussen and S.J. Knak Jensen, Phys. Rev. **B24**, 2744 (1980).

³¹ W. Selke, D. Catrein, and M. Pleimling, J. Phys. A **33**, L459 (2000).

³² G. Gumbs, Phys. Rev. **B33**, 6500 (1986).

³³ K. Binder and H.L. Frisch, Eur. Phys. J. B **10**, 71 (1999).

³⁴ H.L. Frisch, J.C. Kimball, and K. Binder, J. Phys. Condens. Matter **12**, 29 (2000).

³⁵ D.P. Landau, R. Panday, and K. Binder, Phys. Rev. **B39**, 12302 (1989).

³⁶ P.D. Beale, P.M. Duxbury, and J.M. Yeomans, Phys. Rev. **B31**, 7166 (1985).

³⁷ K. Binder and J.-S. Wang, J. Stat. Phys. **55**, 87 (1989); K.-t. Leung, Phys. Rev. Lett. **66**, 453 (1991).

³⁸ M. Pleimling and W. Selke, Eur. Phys. J. B **1**, 385 (1998).

³⁹ U. Wolff, Phys. Rev. Lett. **62**, 361 (1989).

⁴⁰ M. Henkel and M. Pleimling, cond-mat/0108454.

⁴¹ E. Luijten and H.W.J. Blöte, Int. J. Mod. Phys. C **6**, 359 (1995).

⁴² V.S. Dotsenko, W. Selke, and A.L. Talapov, Physica A **170**, 278 (1991).

⁴³ K. Kaski and W. Selke, Phys. Rev. **B31**, 3128 (1985).

⁴⁴ U. Ritschel and P. Czerner, Phys. Rev. Lett. **77**, 3645

(1996).

⁴⁵ C. Ruge and F. Wagner, Phys. Rev. **B52**, 4209 (1995).

TABLE I. Bulk critical temperatures obtained for different values of the bulk competition parameter κ_b .

κ_b	0.15	0.24	0.27
$k_B T_c / J_b$	4.131 ± 0.004	3.865 ± 0.003	3.7475 ± 0.0005

TABLE II. Surface critical exponents at the bulk Lifshitz point obtained for the 3D semi-infinite ANNNI model with the surface layer oriented perpendicular to the axial direction. OT-MF: mean-field exponents at the ordinary transition³³, OT-MC: Monte Carlo values at the ordinary transition, SP-MC: Monte Carlo values at the special transition point. The numbers in brackets give the estimated error in the last digit.

	β_1^L	γ_1^L	γ_{11}^L	β_s^L	γ_s^L
OT-MF	1	1/2	-1/4	1/4	5/4
OT-MC	0.618(5)	0.84(5)	-0.06(2)	-0.14(4)	1.69(7)
	$\beta_{1,sp}^L$	$\gamma_{1,sp}^L$	$\gamma_{11,sp}^L$		
SP-MC	0.22(2)	1.28(8)	0.76(5)		

TABLE III. The same as in Table II, but now for the 3D semi-infinite ANNNI model with the surface layer oriented parallel to the axial direction. Mean-field values are extracted from Ref.³⁴. The mean-field values of the critical exponents β_s^L and γ_s^L , which are not given in Ref.³⁴, follow from the assumption that the scaling relations (14) and (15) hold.

	β_1^L	γ_1^L	γ_{11}^L	β_s^L	γ_s^L
OT-MF	1	1/2	-1/2	0	3/2
OT-MC	0.687(5)	0.82(4)	-0.29(6)	-0.46(3)	1.98(8)
	$\beta_{1,sp}^L$	$\gamma_{1,sp}^L$	$\gamma_{11,sp}^L$		
SP-MC	0.23(1)	1.30(6)	0.72(4)		

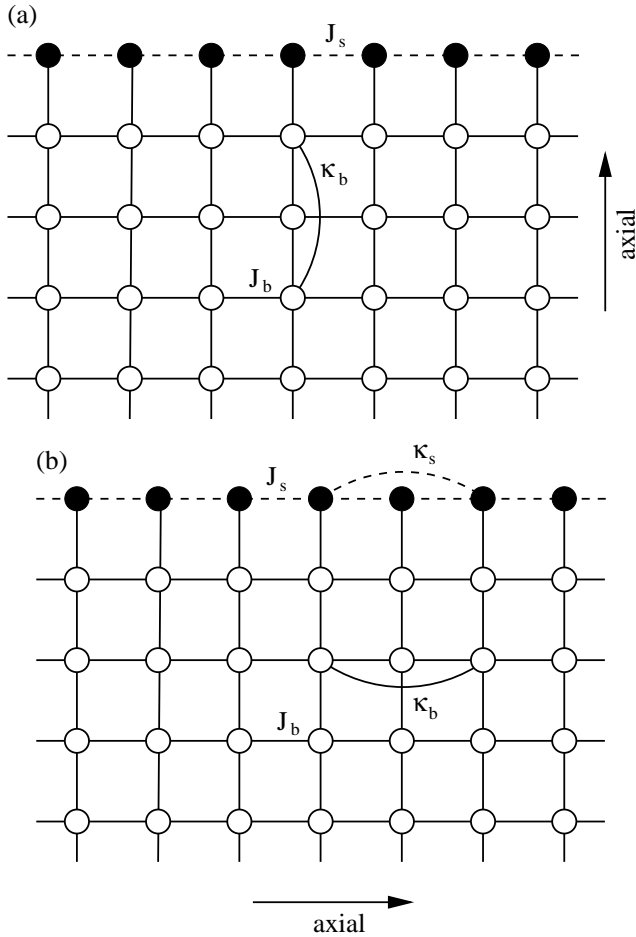


FIG. 1. Cross sections of semi-infinite three-dimensional ANNNI models showing the two different types of surfaces studied in the present work: (a) surfaces perpendicular to the axis of competing interactions, (b) surfaces parallel to this axis. J_b and J_s denote the nearest neighbor bulk and surface couplings, respectively, whereas the axial next-nearest neighbor interactions are labeled by the bulk, κ_b , and surface, κ_s , competition parameters. Surface lattice sites are represented by filled points.

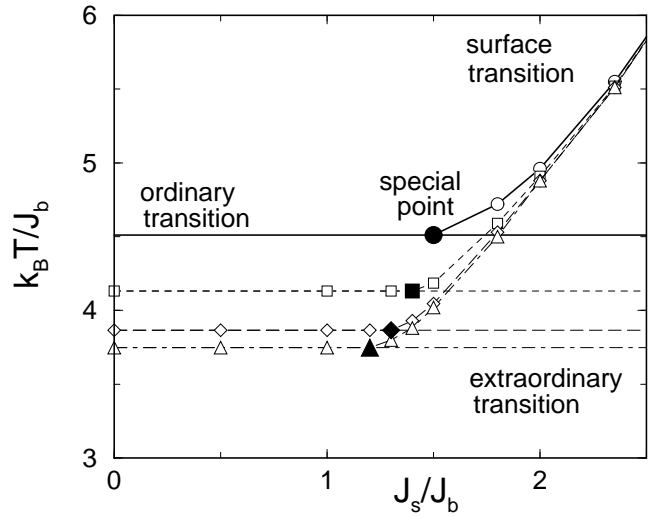


FIG. 2. Surface phase diagrams obtained for different values of the bulk competition parameter κ_b : 0 (circles), 0.15 (squares), 0.24 (diamonds), and 0.27 (triangles). Computed critical temperatures are shown as symbols, the filled symbols indicate the locations of the different special transition points. The shift in the bulk critical temperatures (horizontal lines) as a function of κ_b is obvious. Note that for the Lifshitz point value of κ_b ($\kappa_b^L = 0.27$) a special transition point and a surface transition line are still encountered.

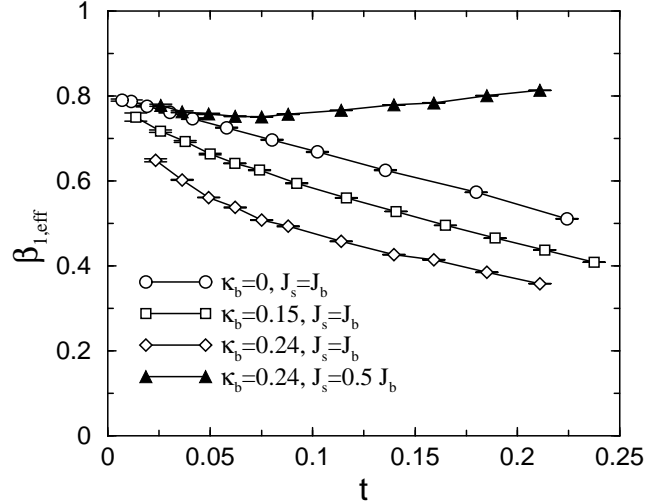


FIG. 3. Surface magnetization effective exponents as function of the reduced temperature t for different interaction sets as indicated in the legend. Note that in the limit $t \rightarrow 0$ all curves extrapolate to the common asymptotic value $\beta_1 \approx 0.80$, thus demonstrating that the ordinary transitions encountered for these interaction sets all belong to the same Ising surface universality class. In order to avoid finite-size dependences Monte Carlo systems with up to $120 \times 120 \times 40$ spins have been simulated. Error bars result from averaging over at least ten different realizations.

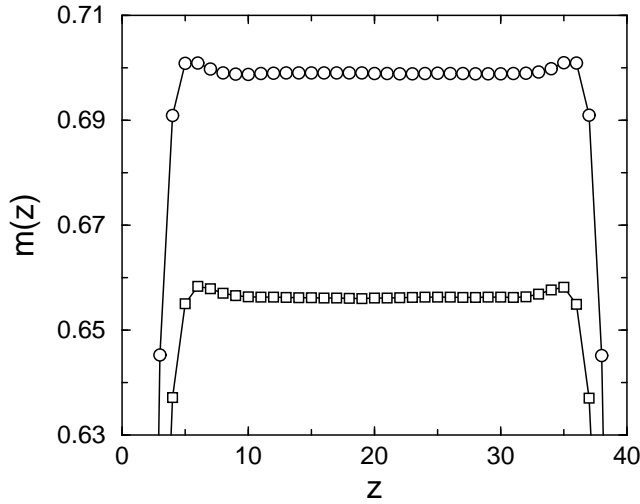


FIG. 4. Layer magnetizations obtained in the Monte Carlo simulation of an ANNNI film containing $120 \times 120 \times 40$ spins, with $\kappa_b = \kappa_b^L$ and $J_s = 0.75J_b$. The two data sets correspond to two different temperatures: $k_B T / J_b = 3.55$ (circles) and $k_B T / J_b = 3.60$ (squares). Shown is the most interesting part where a non-monotonic behaviour as function of the layer index is observed. The error bars are far smaller than the sizes of the symbols.

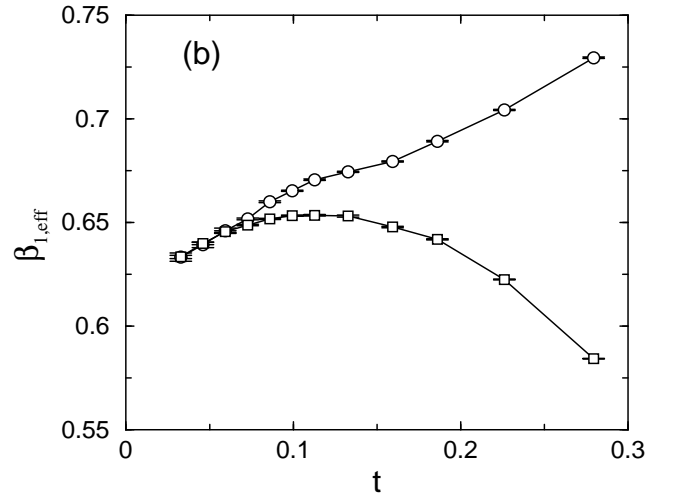
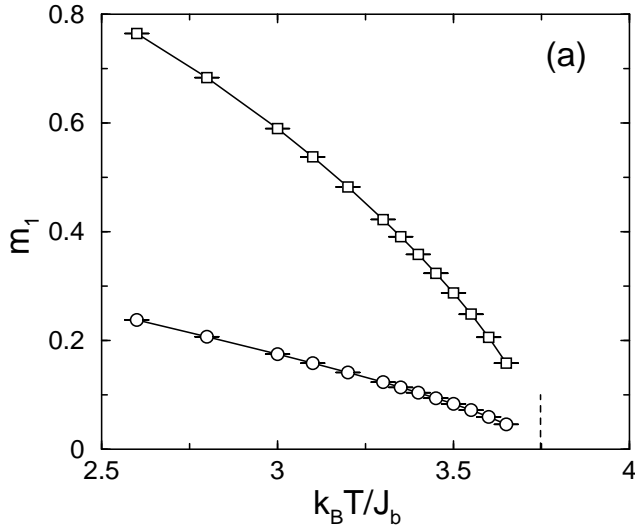


FIG. 5. (a) Surface magnetization versus temperature and (b) effective exponent $\beta_{1,eff}$ versus t for $\kappa_b = \kappa_b^L$. The data shown have been obtained for two values of the surface couplings: $J_s = 0$ (circles) and $J_s = 0.75J_b$ (squares). A linear extrapolation of the effective exponents close to $t = 0$ yields the estimate $\beta_1 = 0.618 \pm 0.005$ for the surface magnetization critical exponent at the Lifshitz point. In (a) the dashed line indicates the Lifshitz point critical temperature $k_B T_c^L / J_b = 3.7475$. Only data not affected by finite-size effects are shown. Systems with up to $120 \times 120 \times 60$ spins have been simulated.

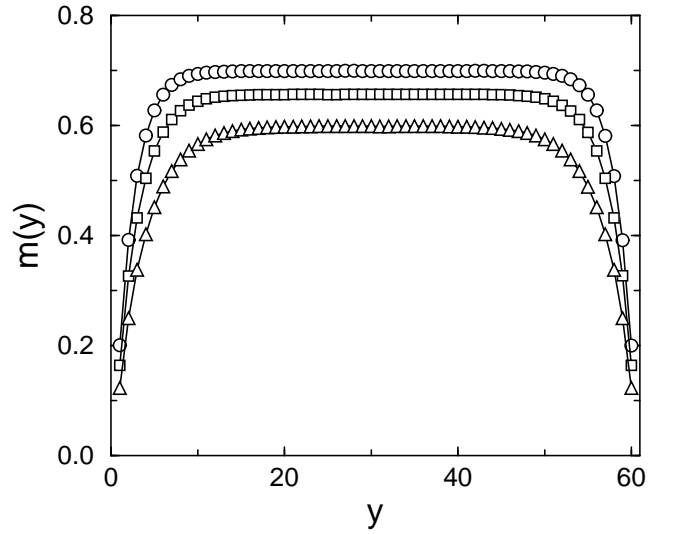


FIG. 6. Layer magnetizations computed for ANNNI samples with surfaces parallel to the axial direction at different temperatures: $k_B T / J_b = 3.55$ (circles), $k_B T / J_b = 3.60$ (squares) and $k_B T / J_b = 3.65$ (triangles). Films with $60 \times 60 \times 60$ spins have been simulated, with $\kappa_s = \kappa_b = \kappa_b^L$ and $J_s = J_b$. The layer magnetization increases monotonically with the distance to the surface. Error bars are far smaller than the sizes of the symbols.

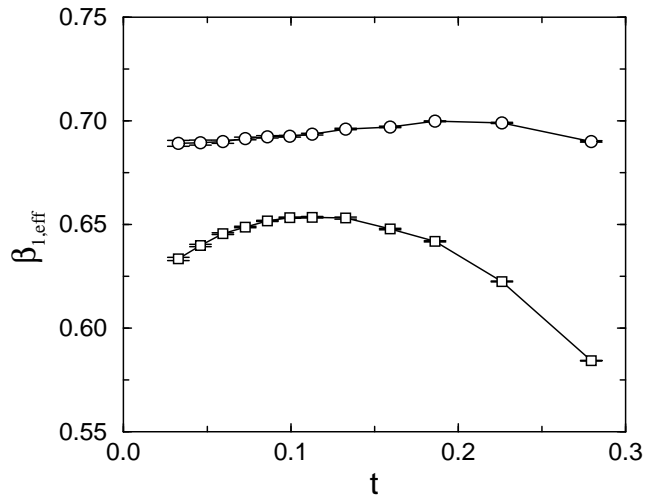


FIG. 7. Comparison of surface magnetization effective exponents obtained at the bulk Lifshitz point from ANNNI samples with different surface orientations: surface perpendicular to the axial direction (squares) or parallel to that axis (circles). In the former case $J_s = 0.75J_b$, whereas in the latter case $\kappa_s = \kappa_b = \kappa_b^L$ and $J_s = J_b$. Extrapolating these data to $t = 0$ yields different values for the Lifshitz point surface magnetization critical exponent at the ordinary transition. In order to circumvent finite-size effects, different system sizes have been simulated. The largest system considered contained $120 \times 120 \times 60$ spins (squares) or $80 \times 80 \times 80$ spins (circles), respectively.